

1 Supplementary material for

2

3 **Late Pleistocene records of speleothem stable isotopic compositions from Pinnacle Point on the South**  
4 **African south coast**

5

6 Kerstin Braun<sup>a,b,c\*</sup>, Miryam Bar-Matthews<sup>a</sup>, Alan Matthews<sup>b</sup>, Avner Ayalon<sup>a</sup>, Richard M. Cowling<sup>d</sup>,  
7 Panagiotis Karkanas<sup>e</sup>,  
8 Erich C. Fisher<sup>c</sup>, Kelsey Dyez<sup>f</sup>, Tami Zilberman<sup>a</sup>, Curtis W. Marean<sup>c,d</sup>

9

10 <sup>a</sup>Geological Survey of Israel, Jerusalem, Israel

11 <sup>b</sup>Fredy and Nadine Herrmann Institute of Earth Sciences, Hebrew University of Jerusalem, 91904  
12 Jerusalem, Israel

13 <sup>c</sup>Institute of Human Origins, School of Human Evolution and Social Change, Arizona State University,  
14 Tempe, Arizona 85287, USA

15 <sup>d</sup>African Centre for Coastal Palaeoscience, Nelson Mandela University, Port Elizabeth, South Africa

16 <sup>e</sup>The Malcolm H. Wiener Laboratory for Archaeological Science, American School of Classical Studies,  
17 Athens, Greece

18 <sup>f</sup>Lamont-Doherty Earth Observatory, Columbia University, Palisades, New York, USA

19

20 \*corresponding author contact: kerstin.braun@mail.huji.ac.il

21

22 **Supplementary Chapter 1: Description of sample material**

23

24 Speleothem samples originated from two sites at Pinnacle Point which were located about 230m apart.  
25 The new records include five samples from Staircase Cave and six samples from PP29.

26

27 Staircase Cave

28

29 *46322*

30 Sample 46322 is a piece of flowstone that was drilled with a 5 cm diameter core bit. The layer of  
31 speleothem is up to 5 cm thick and has a beige to light brown color with indistinct white lamination. One  
32 thick white lamina can be seen close to the top of the sample (8.5 mm depth) and one distinct but  
33 thinner white lamina is located at the center of the sample (27 mm, Supplementary Figure 1f). Twelve  
34 ages were analyzed on the sample giving results between  $394.8 \pm 15.3$  ka (B1) and  $206.8 \pm 2.1$  ka (A1,  
35 Supplementary Figure 1a, Figure 2a, Table 1). The initial StalAge age modelling did not find any major  
36 outliers but several age reversals are present in the sample leading to minor outliers (A1, A5, B1). All  
37 these outliers were drilled very close to white laminae in the sample, two of which represent hiatuses  
38 and therefore may have been affected by diagenetic effects. An initial linearly interpolated age model  
39 was constructed excluding the minor outliers and reveals two sections in the sample in which the  
40 growth rate is reduced from the common 0.42 – 2.0 mm/ka to 0.16 and 0.24 mm/ka, both these  
41 sections also show white laminae indicating hiatuses at 27 and 46 mm depth (Supplementary Figure 1a).  
42 The small section below the hiatus at 46 mm was dated only by one age and therefore no age model can  
43 be constructed. Four ages in the section between 46 and 28 mm depth were used for age model  
44 construction (excluding the outlier B1). The linear interpolation (276.6 – 247.8 ka) and StalAge (290.3 –  
45 241.6 ka) differ mainly in the extrapolation of ages in the oldest part of the age model (Figure 2a). Four  
46 ages were used for the age model construction in the upper 27 mm of the sample (excluding outliers A1  
47 and A5). The linear interpolation (243.0 – 206.2 ka) and StalAge (239.2 – 207.6 ka) age models overlap  
48 well (Figure 2a, Supplementary Table 1).

49 The  $\delta^{18}\text{O}_c$  values of this sample between ~218 and 208 ka show an opposite trend than four other  
50 samples covering this time interval (46330-1, 46861, 142819, and 142820). 46322 was therefore  
51 excluded from the composite record.

52

53 *46330*

54 Sample 46330 is about 8 cm high and 3.5 cm wide. A central speleothem is overgrown at the base by a  
55 bulge of younger material, possibly a pool rim deposit (Supplementary Figure 1 b). The central

56 speleothem and the overgrowth were sampled in two separate sections and separate age models,  
57 46330a and 46330b, were therefore constructed.

58 The central section of the speleothem was dated by 14 ages. 13 of these ages are very close together  
59 between  $219.2 \pm 5.1$  (a) and  $209.3 \pm 4.2$  ka (a4) and overlap within their error ranges. One age (B5: 107.8  
60 ka, 29.5 mm depth) was identified by StalAge as a major outlier and disregarded in the linear  
61 interpolation age model. The growth rate of 46330a varies from 2.2 mm/ka at the base of the sample to  
62 between 10 and 48 mm/ka in the upper sections. There is no indication of a hiatus. The linear  
63 interpolated age model covers the time interval between 217.6 and 210.2 ka and overlaps well with the  
64 StalAge age model (217.6 – 210.2 ka, Figure 2b, Supplementary Table 1).

65 The second isotopic record, 46330b, was analyzed on the overgrowth at the base of the sample  
66 (Supplementary Figure 1c). Four ages were analyzed in this section with results in stratigraphic order  
67 between  $202.5 \pm 1.8$  (H) and  $175.6 \pm 5.9$  ka (E). The linear interpolation and StalAge age models give  
68 very similar results (Figure 2c) covering the intervals from 205.0 to 173.9 ka and from 205.0 to 176.0 ka,  
69 respectively (Supplementary Table 1). For consistency, the linear interpolation age model was used.

70

71 *46861*

72 Sample 46861 was drilled with a 5cm diameter core bit and is about 6.5 cm high. The color of the  
73 speleothem changes from grey at the base to dark brown to lighter brown at the top. Two distinct white  
74 lamina cut across the sample at about 43 and 8.5 mm depth (Supplementary Figure 1d) .

75 11 dating analyses run on the sample gave results between  $310.6 \pm 18.6$  ka (C1) and  $183.3 \pm 4.1$  ka (A).  
76 Within their error ranges, all ages were in stratigraphic order (Figure 2d) and StalAge therefore does not  
77 detect any outliers. An initial linear interpolation age model has growth rates between 0.2 and 4.5  
78 mm/ka. The lowest growth rates were measured at the base of the sample between 66 – 62 mm depth,  
79 at 46 to 55 mm depth and close to the top between 7 and 11 mm depth. The isotopic record does not  
80 extend into the section at the very base of the sample (66-63 mm depth) so we will not further  
81 investigate this section. A minor change in the texture and color of the speleothem in the depth interval  
82 between 46 and 55 mm indicates a possible hiatus at 51 mm depth. The white line at 8.5 mm depth lies  
83 within the third region of low growth rates and therefore most likely represents another hiatus  
84 (Supplementary Figure 1d). For the final linear interpolation age model, the sample is thus subdivided  
85 into three growth phases, two of which could also be modelled using StalAge. The youngest growth  
86 phase (8 – 2 mm depth) was only dated by two age analyses and therefore could not be modelled with  
87 StalAge.

88 The final age model covers the interval between 309.1 and 256.6 ka, 240.5 to 202.6 ka and 191.0 to  
89 173.1 ka (Supplementary Table 1). There is only minor discrepancy to the StalAge age models for the  
90 lower two growth phases in the depths between 38 and 51 mm, but the final linear interpolation age  
91 model remains within the 95% confidence limits of StalAge (Figure 2d).

92

93 *50100*

94 Sample 50100 is a flowstone that was drilled with a 5 cm diameter core drill and is ~ 5 cm high. The  
95 sample has a light beige to yellow color with little visible lamination (Supplementary Figure 1 e). Seven  
96 age analyses gave results between  $238.7 \pm 3.7$  ka (1) and  $194.4 \pm 2.2$  ka (3) and where all in stratigraphic  
97 order. Growth rates vary between 7.5 and 0.3 mm/ka, but there is no indication for a hiatus in the  
98 sample. Continuous age models were therefore constructed using linear interpolation and StalAge; the  
99 age models show good overlap covering the intervals from 245.9 to 193.9 ka and from 242.4 to 192.5 ka,  
100 respectively (Figure 2 e, Supplementary Table 1)

101

102 *142819*

103 Sample 142819 is about 12 cm high and 10 cm wide. ~4.5 cm at the bottom of the sample consists of  
104 porous tufa with a reddish brown color (Supplementary Figure 1f). The flowstone grew on top of this  
105 tufa. The 3.5 cm at the base of the flowstone is light grey to beige in color but then changes abruptly to  
106 brown. Thin white lamination can be seen at the boundary between the light grey and brown parts. A  
107 petrographic thin section was prepared of the boundary area between the two colors (blue line in  
108 Supplementary Figure 1f). The area below the abrupt color change consists of large several mm long and  
109 up to 0.5 mm wide crystals with an elongated columnar fabric (Supplementary Figure 4 a, b). The  
110 boundary between the two differently colored areas in the thin section is marked by an open pore  
111 which almost seems continuous though the thin section (Supplementary Figure 4 a, b). In the sample  
112 this pore corresponds to a white lamina (~37.5 mm depth, Supplementary Figure 1f), which may consist  
113 of softer material that was eroded during the preparation of the thin section. This layer most certainly  
114 represents a hiatus. The crystals succeeding the open pores are also elongated with a columnar fabric  
115 but further towards the top of the sample, they change to a more needle like crystal shape  
116 (Supplementary Figure 4 b, c).

117 Thirteen ages were measured on sample 142819, ranging from  $312.8 \pm 5.5$  ka (C1) to  $129.9 \pm 1.1$  ka (A).  
118 An initial age model by StalAge identifies one major outlier (B:  $185.3$  ka  $36.0$  mm depth). This dating  
119 sample was drilled just above the major color change in the sample and might be offset due to  
120 contamination by the hiatus. A second sample (C:  $233.4$  ka  $40$  mm depth) was drilled just below the  
121 hiatus layer and is therefore also considered to be an outlier, although it was not recognized by StalAge.  
122 A third age at  $48$  mm depth (C1:  $311.3 \pm 6.2$  ka) is older than suggested by the ages around it but  
123 overlaps within error with an age measured at  $54$  mm depth (C1:  $301 \pm 6$  ka). This age is considered a  
124 minor outlier and not included in the age model. An initial age model was linearly interpolated between  
125 the remaining 10 ages and growth rates range between  $3.2$  mm/ka and  $0.1$  mm/ka. The lowest growth  
126 rates were found in the section containing the previously identified hiatus and between  $9$  and  $13.5$  mm  
127 depth. There is no color change or lamination indicating a hiatus in the latter section but a steep change  
128 in the  $\delta^{18}\text{O}_c$  and  $\delta^{13}\text{C}$  ( $1\text{‰}$  and  $3\text{‰}$ , respectively) between  $9$  and  $10$  mm depth suggests a hiatus at this  
129 depth.

130 For the final age model, the sample was subdivided into three growth sections at 9 and 37.5 mm depth  
131 (Figure 2f). The oldest section of the sample was dated five times, but two ages were outliers. There is a  
132 discrepancy between the linear interpolation (304.1 – 268.8 ka) and the StalAge age model (313.6 –  
133 299.9 ka) since StalAge does not recognize the age at 48mm depth (C1) as an outlier. The second growth  
134 phase was dated by 5 ages. The outlier at 36 mm depth was recognized by StalAge and the linear  
135 interpolation (237.3 - 175.7 ka) and StalAge (237.6 – 177.9 ka) age models overlap very well. The  
136 uppermost 9 mm of the sample were dated by 3 ages, however due to a change in growth rate from 3.1  
137 to 0.2 mm/ka StalAge was not able to construct an age model. The linear interpolation age model covers  
138 the interval between 141.0 and 129.6 ka (Figure 2f, Supplementary Table 1).

139

140 *142820*

141 Sample 142820 is a 5 cm long piece of flowstone with a light brown to olive green color (Supplementary  
142 Figure 1g). A white lamina is visible at 14 mm depth. A thinner white line is visible at about 30 mm depth  
143 (Supplementary Figure 1g). Eight ages were measured on the sample and gave results between  $321.7 \pm$   
144  $6.4$  ka and  $167.0 \pm 2.7$  ka in stratigraphic order (Figure 2h). No outliers were therefore detected by the  
145 initial StalAge age model. The growth rate of the initial linear interpolated age model varies between 0.1  
146 and 2.8 mm/ka. Growth rates below 0.3 mm/ka were found in three regions in the sample: 43 – 33.5  
147 mm depth, 29 – 25 mm depth and 15.5 - 11.5 mm depth. The white lamina at 14mm depth is within the  
148 uppermost section with a low growth rate, which indicates that it represents a hiatus. The other two  
149 sections with slow growth do not show any signs of a hiatus and continuous growth was therefore  
150 assumed. The sample was subdivided into two growth sections between 44.5 and 14.5 mm and from 14  
151 to 0.5 mm depth. The growth section between 44.5 and 14.5 mm depth was dated by 6 analyses. The  
152 linear interpolation age model (334.3 – 207.7 ka) and the StalAge (299.3 – 207.9 ka) age models deviate  
153 from each other close to the base of the sample, but the linear interpolation age model always remains  
154 within the 95% confidence limit of the StalAge age model (Figure 2g, Supplementary Table 1). The upper  
155 growth section between 14 and 0.5 mm depth was dated only by two ages and therefore could not be  
156 modelled with StalAge. The linear interpolation age model covers the interval between 195.5 and 160.9  
157 ka (Figure 2 g, Supplementary Table 1).

158

159 *PP29*

160

161 *46745*

162 Sample 46745 is ~7 cm long dark brown speleothem intercalated with thin white laminae. The  
163 speleothem is embedded between two aeolianite layers (Supplementary Figure 2a). Five ages measured  
164 on the sample gave results between  $111.2 \pm 1.2$  ka (A1) and  $71.7 \pm 0.8$  ka (B) and (Figure 3a,  
165 Supplementary Figure 2a, Table 1). Initial StalAge and linear interpolation age models overlap well

166 (Figure 3a). The StalAge age model identifies the age close to the bottom of the sample (A: 104.9 ka, 69  
167 mm) as a major outlier. This sample was drilled close to the boundary with the sand deposit that  
168 surrounds this sample and might have been contaminated. The initial linear interpolation age model  
169 covers the interval between 112.6 and 64.7 ka with growth rates between 12.8 and 0.5 mm/ka. The  
170 interval with the lowest growth rate (0.5 mm/ka) between 34 and 18.5 mm depth also contains a thick  
171 white wavy lamina below an unconformity in the lamination at ~ 24 mm depth. It is therefore assumed  
172 that there is a hiatus at this depth in the sample and the sample was subdivided into two growth  
173 sections below and above 24 mm depth. Each of the growth sections was dated only by two dating  
174 analyses and StalAge age modelling was therefore not possible. The final linear interpolation age models  
175 cover the periods from 112.6 to 108.3 ka and 93.5 to 64.7 ka (Supplementary Table 1). The final age  
176 model differs from the initial StalAge age model only in the sections close to the hiatus and remains  
177 within the 95% confidence limit even where there is deviation (Figure 3a).

178

179 *46746*

180 Sample 46746 is a ~26 cm long and ~7.5 cm wide stalactite (Supplementary Figure 2b). The color of the  
181 sample is dark brown to olive with a few interspersed white laminae. The sample is overgrown on one  
182 side by a thin (few mm) layer of white laminated speleothem.

183 The ages measured on sample 46746 range between  $104.9 \pm 0.8$  ka (A3) and  $46.4 \pm 0.3$  ka (D). The  
184 youngest age (D: 46.4 ka) was measured on the white overgrowth on one side of the sample  
185 (Supplementary Figure 2b) which is likely a second growth phase separated from the remainder of the  
186 sample by a hiatus. Since only one age could be measured on this thin layer, it is excluded from the age  
187 models.

188 The stalactite was sampled perpendicular to its growth axis and ages are younger at both outer edges  
189 and older closer to the center of the sample (Supplementary Figure 2b). We therefore constructed two  
190 age models, 46746a and 46746b, both starting from the center at 33mm depth which has an age of ~99  
191 ka well constrained by two ages (B1:  $98.8 \pm 0.7$  ka at 33.5 mm depth and B:  $99.3 \pm 1.9$  ka at 32 mm  
192 depth). Section 46746a includes the depths in the sample between 0 and 33 mm and section 46746b  
193 includes the depths between 33 and 66 mm. Two ages, sampled ~6 mm from the center of the sample  
194 on either side, gave older results (A3:  $104.9 \pm 0.8$  ka at 27 mm depth and B2:  $100.8 \pm 0.5$  ka at 40 mm  
195 depth) than the two analyses in the center. The initial StalAge age model for section 46746a recognized  
196 age A3 as an outlier (Figure 3b). The remaining four ages in this section of the sample are in stratigraphic  
197 order. StalAge identifies the outermost age (A: 86.1 ka) as a minor outlier since it is offset to younger  
198 age from the other samples. The algorithm creates an age model with a stable growth rate; age A  
199 actually lies outside the 95% confidence limit of this age model (Figure 3b). The linear interpolation age  
200 model for 46746a includes the four ages in stratigraphic order and the young age of sample A leads to a  
201 decrease in growth rate in the outer section (0.7 mm/ka) of the sample compared to the center of the  
202 sample (1.6-4.2 mm/ka). This difference in the treatment of dating samples and growth rate changes

203 leads to an offset between the two age models (Figure 3b). The Linear interpolation age model will be  
204 used and covers the interval between 99.3 and 81.2 ka (Supplementary Table 1).

205 In subsection 46746b, StalAge does not recognize age B2 (100.8 ka) as an outlier. In the initial age model  
206 the algorithm therefore assumes very fast growth at the center of the sample (34.5 to 26 mm depth  
207 ages between 100.9 and 100.2 ka. This initial fast growth is followed by very slow growth between 20  
208 and 26 mm depth which would suggest a hiatus (Figure 3c). However since the age of the center is  
209 confirmed by two dating analyses and the outlier was recognized on the opposite side of the sample  
210 (A3), we assume that age B2 is also an outlier. It was therefore not used in the linear interpolation age  
211 model. The remaining four ages in this section of the sample are in stratigraphic order and growth rates  
212 range between 1.6 and 0.9 mm/ka. The linear interpolation age model does not overlap well with the  
213 initial StalAge age model (Figure 3c). A second StalAge age model (98.6 – 75.2 ka) in which the outlier  
214 was not included overlaps very well with the linear interpolated age model (98.8 – 75.0 ka,  
215 Supplementary Table 1).

216

217 *46747*

218 Sample 46747 is a small piece of drapery speleothem that was cut from the cave ceiling. It is 4 cm long  
219 and 3.5 cm wide and has a light brown color. Three ages were measured on the sample and gave result  
220 of  $143.2 \pm 8.7$  ka (B),  $61.2 \pm 1.6$  ka (C) and  $41.5 \pm 2.1$  ka (A, Supplementary Figure 2c). The oldest age was  
221 located in a section of the sample that was not included in the stable isotopic record. Since there were  
222 only two ages measured at the top and bottom of the isotopic record, StalAge age modelling was not  
223 possible. The linear interpolation age model covers the time between 61.2 and 41.5 ka (Supplementary  
224 Table 1).

225

226 *138862*

227 Sample 138862 is about 30 cm wide and 9 cm high. The sample shows a succession of different cave  
228 deposits with tufa at the base, overlain by a thin layer of laminated speleothem. A layer of aeolianite  
229 overlies the tufa in most of the sample but thins out in the section that we now call 138862.2. The whole  
230 sample is overgrown by clean speleothem mostly overlying the aeolianite, but overlying the laminated  
231 speleothem at the top of the tufa, where aeolianite is not present (Supplementary Figure 2d). The  
232 speleothem is of a light brown or beige to light olive color and shows only few white laminae. The  
233 sample broke into two pieces during cutting; ages and isotopic profiles were analyzed in three positions  
234 on the sample (Supplementary Figure 2e, f).

235 The piece 138862.1 is about 27 cm wide and 7 cm high. The oldest age (C:  $110.5 \pm 0.7$  ka) was analyzed  
236 on the thin layer of laminated speleothem embedded between the tufa and aeolianite at the bottom of  
237 the sample (Supplementary Figure 2e). The section of the clean speleothem on top of the aeolianite was  
238 dated with six ages with results between  $89.0 \pm 0.7$  ka (B) and  $61.1 \pm 0.5$  ka (A). All ages are in

239 stratigraphic order (Figure 3d, Supplementary Figure 2e). The initial interpolated age model results in  
240 growth rates between 15.7 and 0.8 mm/ka. The two sections with the lowest growth rates (1.1 and 0.8  
241 mm/ka) are between 33 and 23 mm and 12 to 3 mm depth. A thick white lamina at 32.5 mm depth  
242 supports a hiatus in the former depth interval, but there is no sign of a hiatus in the latter. For the  
243 section older than the hiatus (60 – 33 mm depth) we linearly interpolated the age model using the three  
244 ages measured on this section of the sample; the resulting age model covers the interval between 89.1  
245 and 86.3 ka and overlaps very well with a second StalAge age model constructed only for this section  
246 (89.4 – 86.4 ka, Figure 3d, Supplementary Table 1). The depth section between 0 and 33 mm was also  
247 dated by three ages, but StalAge age modelling was not possible due to a change in the growth rate  
248 within the section. The linear interpolation age model covers the interval between 79.4 and 58.7 ka  
249 (Supplementary Table 1); apart from the section close to the hiatus this age model is within the 95%  
250 confidence limit of the initial StalAge age model (Figure 3d).

251 Piece 138862.2 is 18 cm wide and 8 cm high. In the section where aeolianite is present, it is overlain by  
252 clean speleothem that is the continuation of the section in 138862.1. Thin white lines indicate that the  
253 speleothem in the lateral part (Supplementary Figure 2f) that directly overlies the tufa represents a  
254 different, older, growth phase. We therefore created two age and isotopic profiles for this piece of the  
255 sample. The profile 138862.2a represents the older speleothem directly overlying the tufa, 138862.2b  
256 was measured on the continuation of the speleothem layer that was also analyzed in 138862.1  
257 (Supplementary Figure 2d-f).

258 Four ages were measured in section 138862.2a and gave results between  $110.2 \pm 0.8$  (D1) and  $103.2 \pm$   
259  $1.3$  ka (C) in stratigraphic order within their error ranges (Figure 3e, Supplementary Figure 2f). StalAge  
260 creates an age model with a stable growth rate which assumes that the age at the base of the sample  
261 (D:  $109.0 \pm 0.7$  ka, 24 mm depth) is an outlier although it overlaps within error with the subsequent age  
262 (D1:  $110.2 \pm 0.8$  ka, 15 mm depth). In the linear interpolation age model we used both ages which leads  
263 to an offset from the StalAge age model (Figure 3e) and a steep change in growth rate from 30 mm/ka  
264 at the base of the sample to 1.3 - 2.4 mm/ka at the top. The final linear interpolation age model covers  
265 the interval between 109.7 and 102.4 ka (Supplementary Table 1).

266 Four ages were measured for section 138862.2b with results between  $84.9 \pm 0.7$  ka (A) and  $90.1 \pm 0.6$  ka  
267 (A1). StalAge recognizes the oldest age in this section (A1) as an outlier (Figure 3f). We therefore  
268 excluded this age from the linear interpolation age model. The interpolated age model covers the  
269 interval between 88.0 and 82.9 ka and overlaps well with the StalAge age model (87.9 – 83.2 ka, Figure  
270 3f, Supplementary Table 1).

271

272 *142828*

273 Sample 142828 is about 8.5 cm high and 5.5 cm wide. Its base is an aeolianite that is overlain by a 4 cm  
274 thick speleothem with a dark brown color at the bottom becoming lighter towards its top  
275 (Supplementary Figure 2g). Thin white lamination can also be seen throughout the speleothem. Nine  
276 ages were measured on the sample and range between  $109.6 \pm 0.9$  ka (A5) and  $50.9 \pm 0.5$  ka (A). StalAge

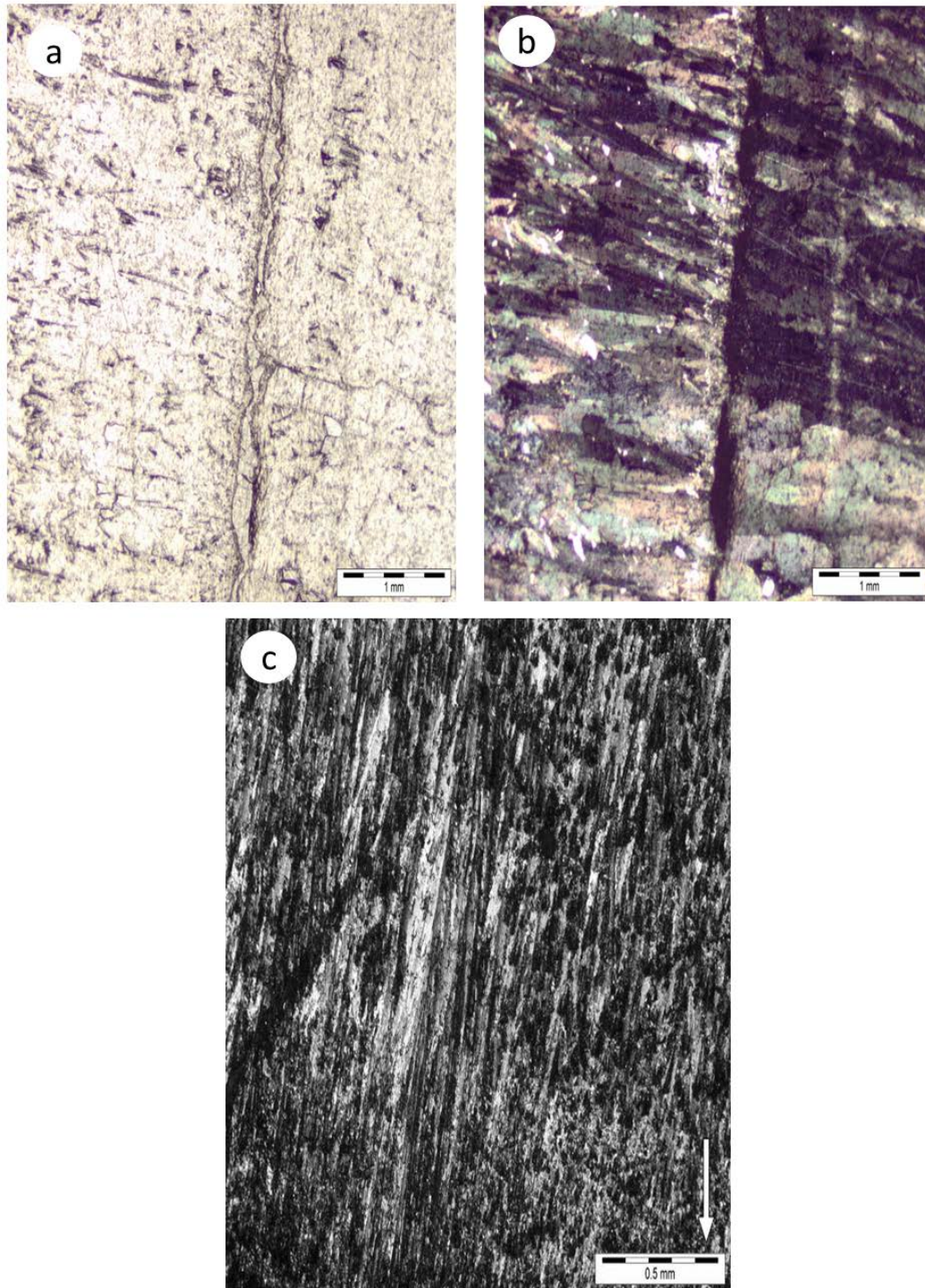
277 recognizes the oldest age measured on the sample (A5) as a major outlier (Figure 3 g). This age is  
278 therefore excluded from the initial linear interpolation age model. Two additional ages (B and C) are  
279 excluded that were measured on a different surface of the sample (rotated by 90°) and gave offset ages  
280 from the surface on which the isotopic record was measured. The remaining six dating analyses gave  
281 result in stratigraphic order within their error ranges. The initial linear interpolation age model shows  
282 major changes in the deposition rate from 10 mm/ka to 0.1 mm/ka. The section with the lowest growth  
283 rate (10 – 6 mm depth) also shows a whiter lamina and a change in color from dark brown in lower parts  
284 to lighter brown in the upper parts. A hiatus is therefore included at 6.5 mm depth. A StalAge age model  
285 constructed for the section below the hiatus used six dating analyses (only excluding the identified  
286 major outlier A5) and covers the interval between 106.4 and 90.7 ka. For the linear interpolation age  
287 model, ages B and C were also excluded, thus four age analyses were used (D, A4, A3, and A2). The age  
288 model overlaps very well with the StalAge age model for this section (Figure 3g) and covers the interval  
289 between 106.3 and 94.1 ka (Supplementary Table 1).

290 The small section above the hiatus was only dated by two age analyses with ages of  $58.3 \pm 0.4$  (A1) and  
291 50.9 ka (A). The interpolated age model for this section covers the interval between 58.3 and 50.9 ka.

292

293

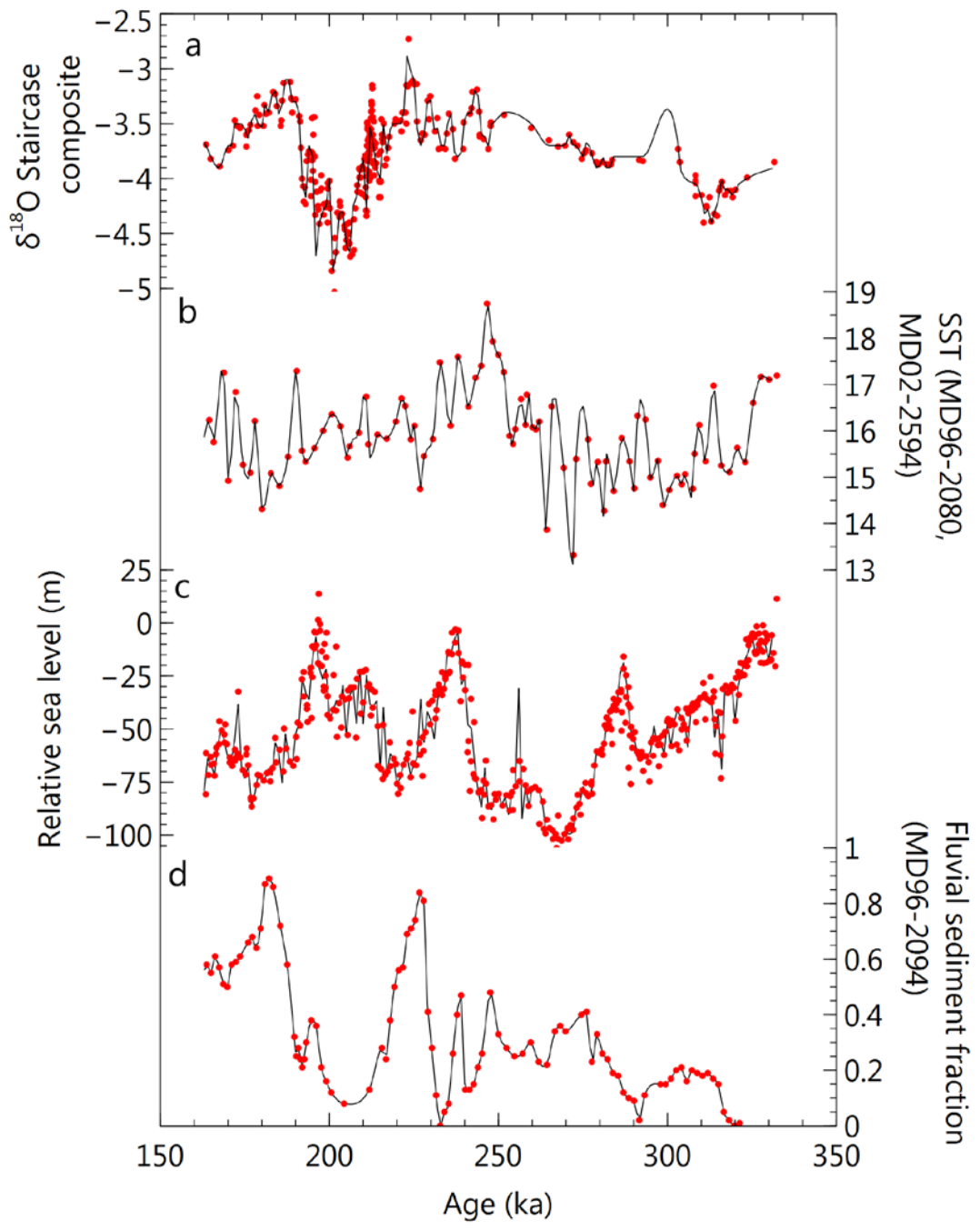
294 **Supplementary Figure 1:** Petrographic images of sample 142819 from Staircase Cave, white arrows  
295 indicate direction of crystal growth; View of the boundary between light gray (right) and brown (left)  
296 material in non-polarized (a) and polarized (b) light. The hiatus is represented by pores at the center of  
297 the images in a and b overgrown by a layer of small crystals. c. needle like carbonate rays in the  
298 youngest part of the thin section.



299

300

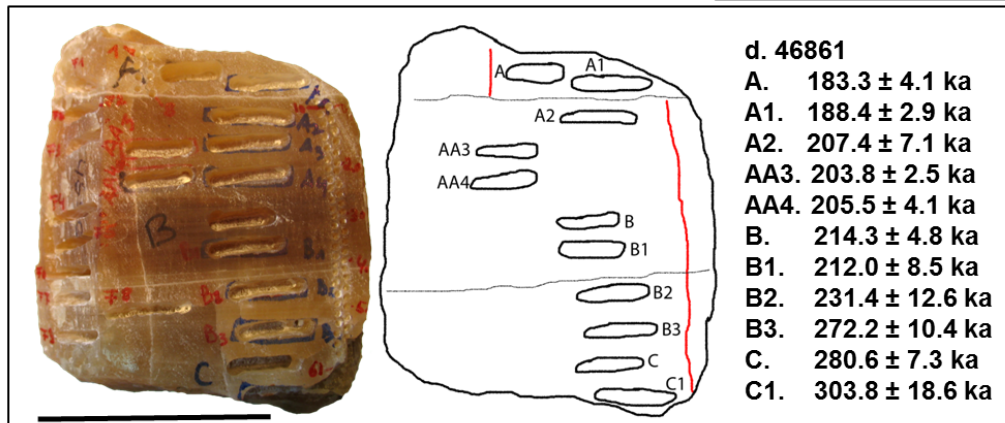
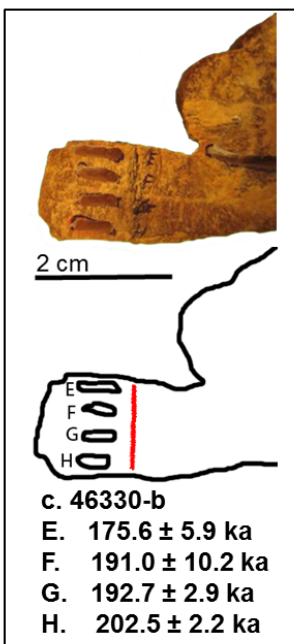
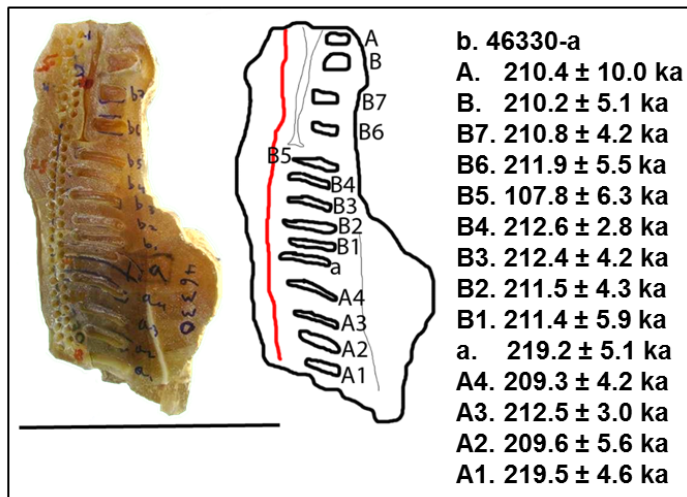
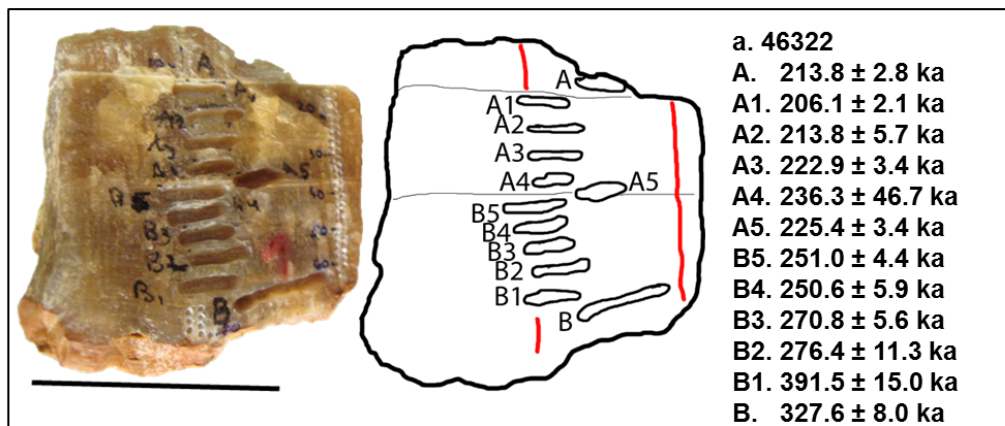
301 **Supplementary Figure 2:** Comparison of the raw data to the cubic spline resampled data used  
302 for the correlation analyses in Figure 6. Red dots mark original analyses, black lines are the resampled  
303 time-series. a. Composite  $\delta^{18}\text{O}_c$  of Staircase Cave between 331 and 164 ka. b. SST record reconstructed  
304 using  $\delta^{18}\text{O}$  of *Globigerina bulloides* from sediment cores MD96-2080 and MD02-2594 (Martínez-Méndez  
305 et al., 2010). c. Relative sea level (Rohling et al., 2009). d. Proportion of fluvial sediment in core MD96-  
306 2094 (Stuut et al., 2002).

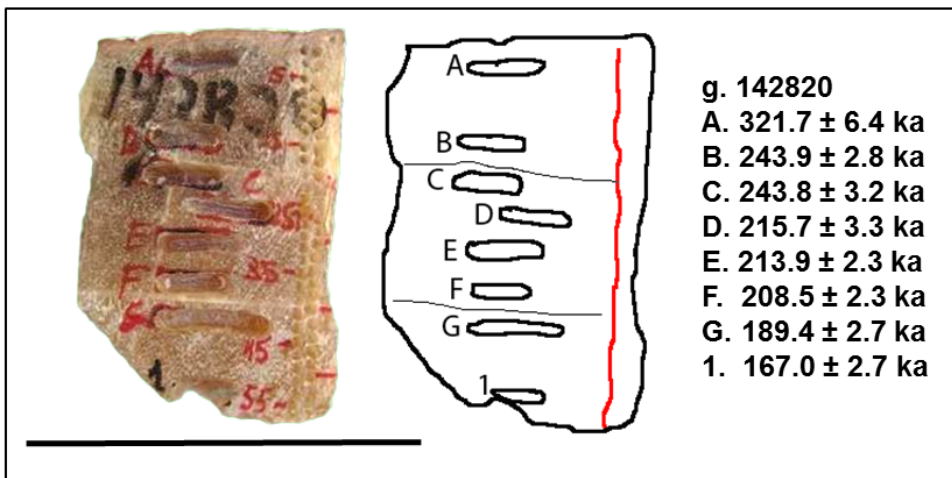
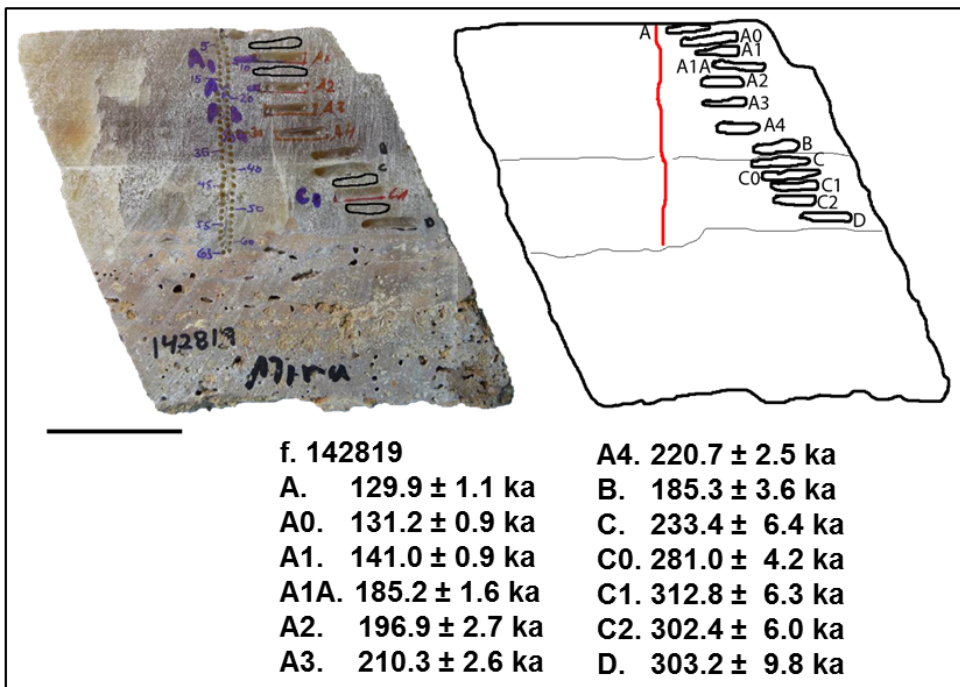
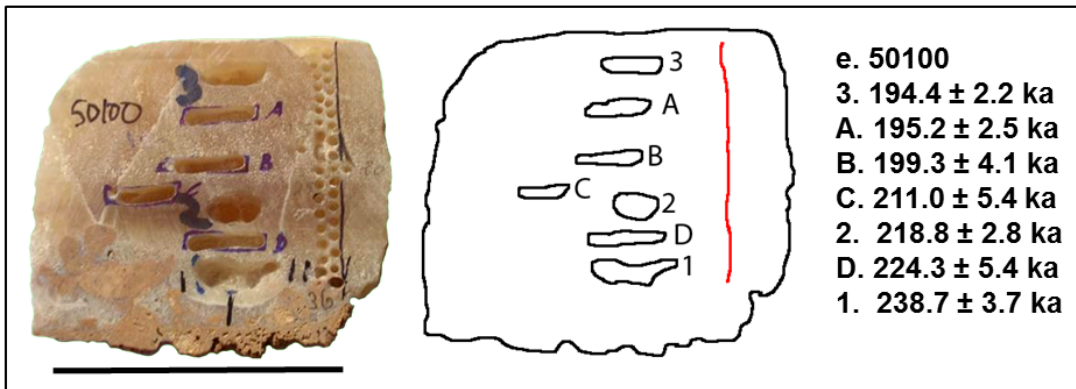


307

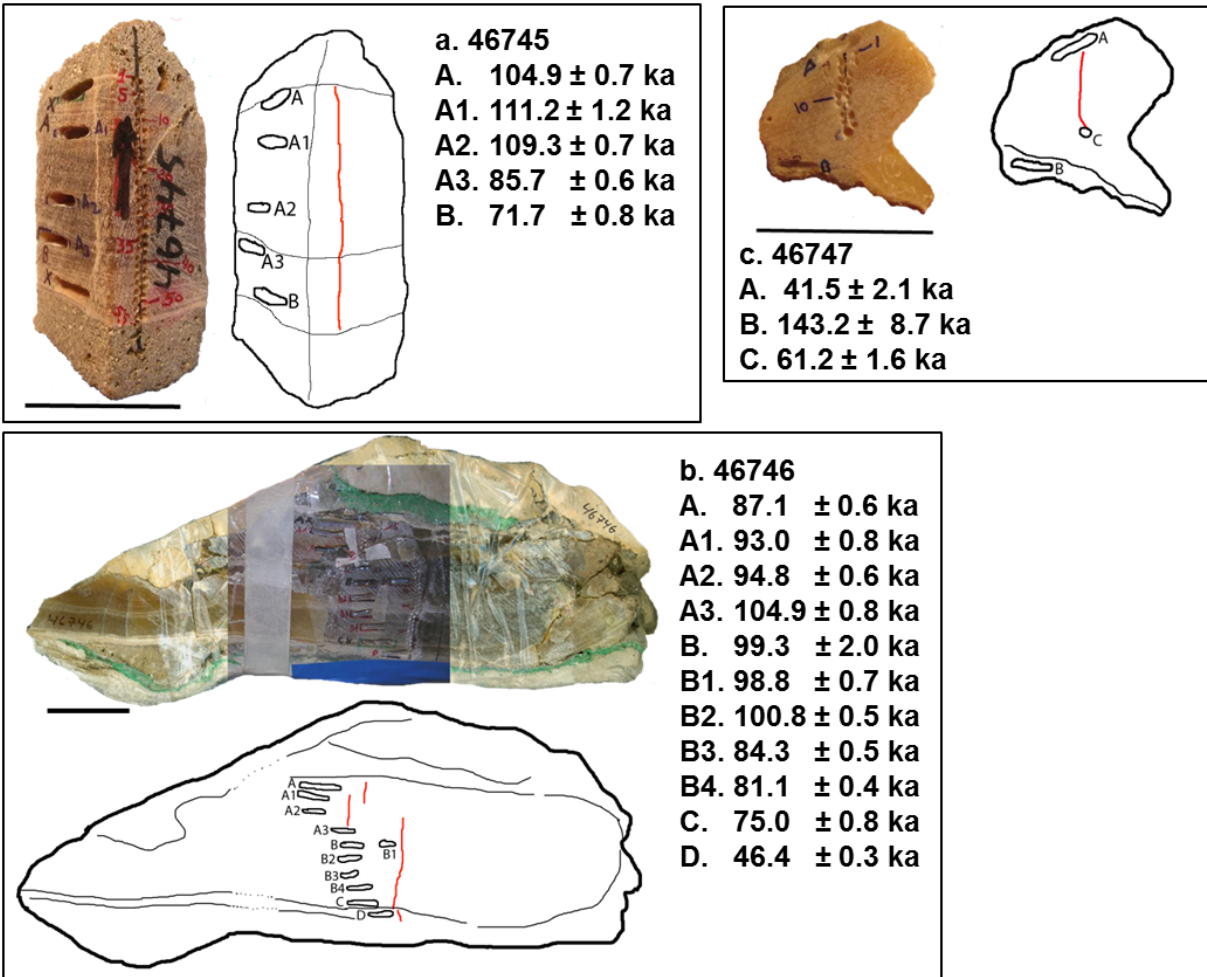
308

309 **Supplementary Figure 3:** Images of samples from Staircase Cave; outlines of samples with locations of  
 310 dating samples (black) and isotopic sections (red) are also shown. Dating results with 2 $\sigma$  errors are given  
 311 for each sample. Black scale bars are 5 cm long, unless stated otherwise.

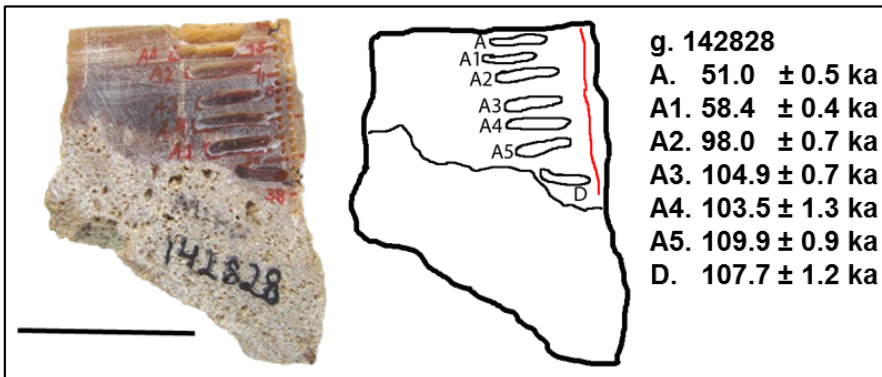
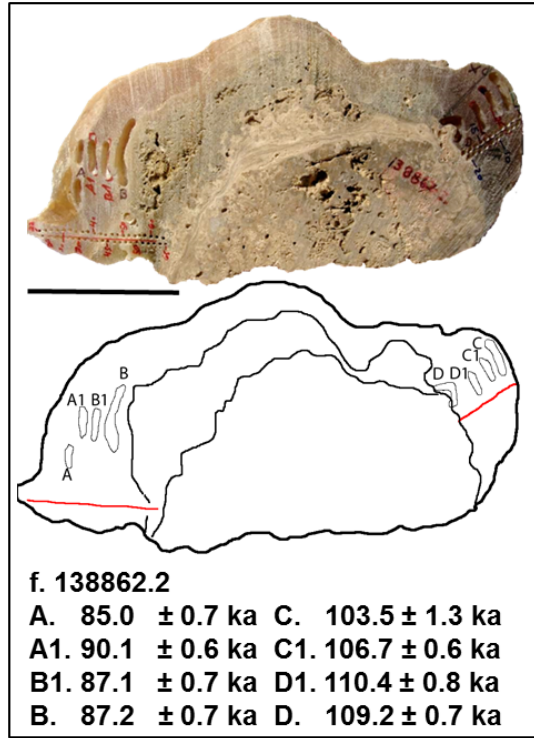
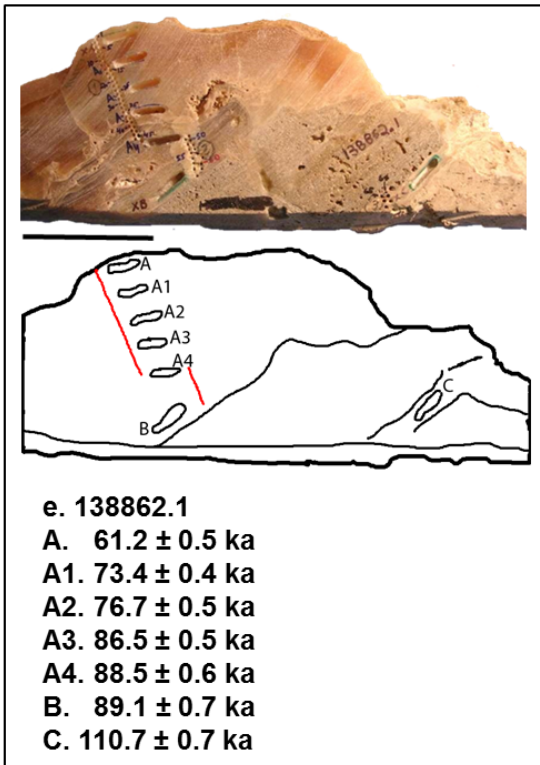




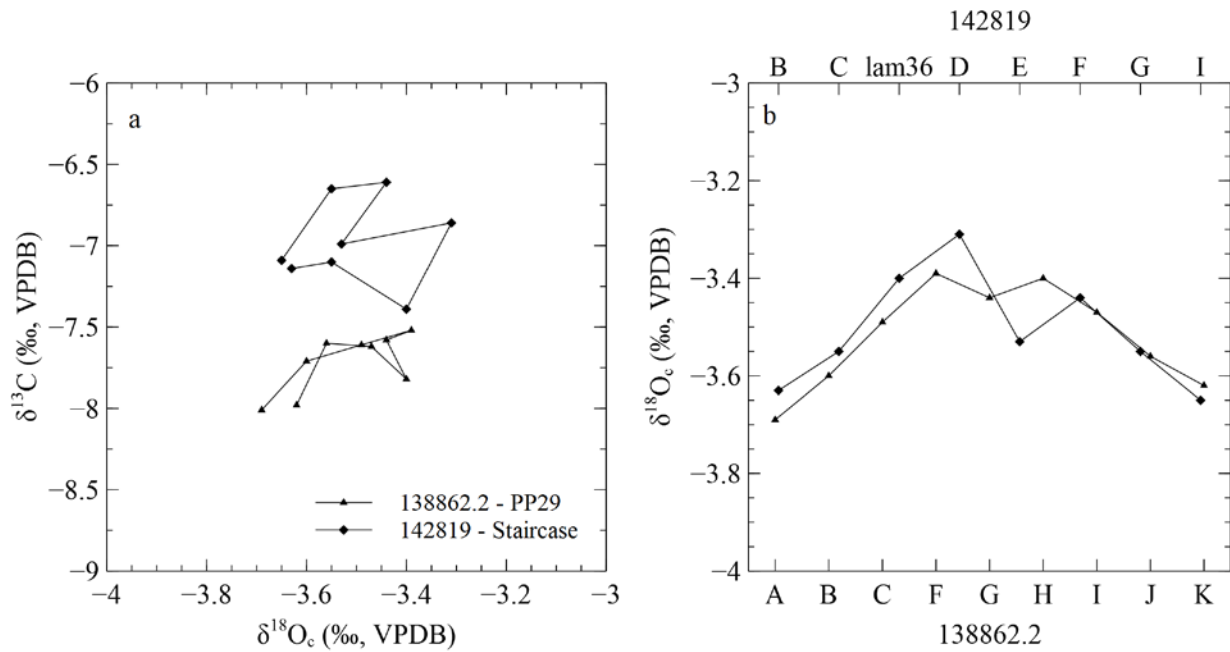
314 **Supplementary Figure 4:** Images of samples from PP29; outlines of samples with locations of dating  
 315 samples (black) and isotopic sections (red) are also shown. Dating results with  $2\sigma$  errors are given for  
 316 each sample. Black scale bars are 5 cm long.



317



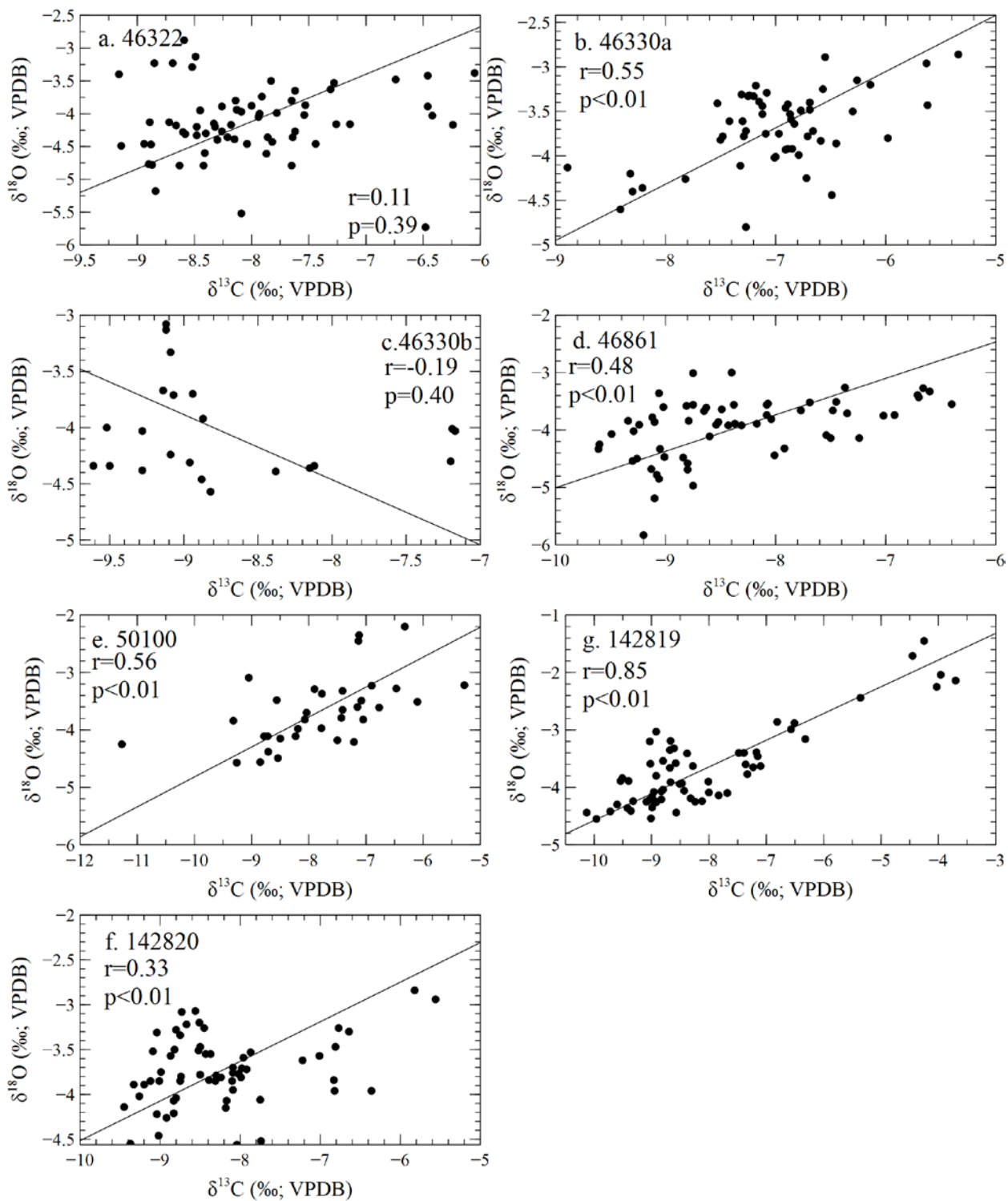
319 **Supplementary Figure 5:** Hendy (1971) Test results for one sample from PP29 (138862.2, triangles) and  
 320 one sample from Staircase Cave (142819, diamonds). a. plot of  $\delta^{18}\text{O}_c$  against  $\delta^{13}\text{C}$  showing there is no  
 321 correlation between the two along the individual lamina. b. plot of  $\delta^{18}\text{O}_c$  against measurement number  
 322 along the lamina (axis for sample 142819 at the top, for 138862.2 at the bottom) showing no  
 323 enrichment of  $\delta^{18}\text{O}_c$  along the lamina.



324

325

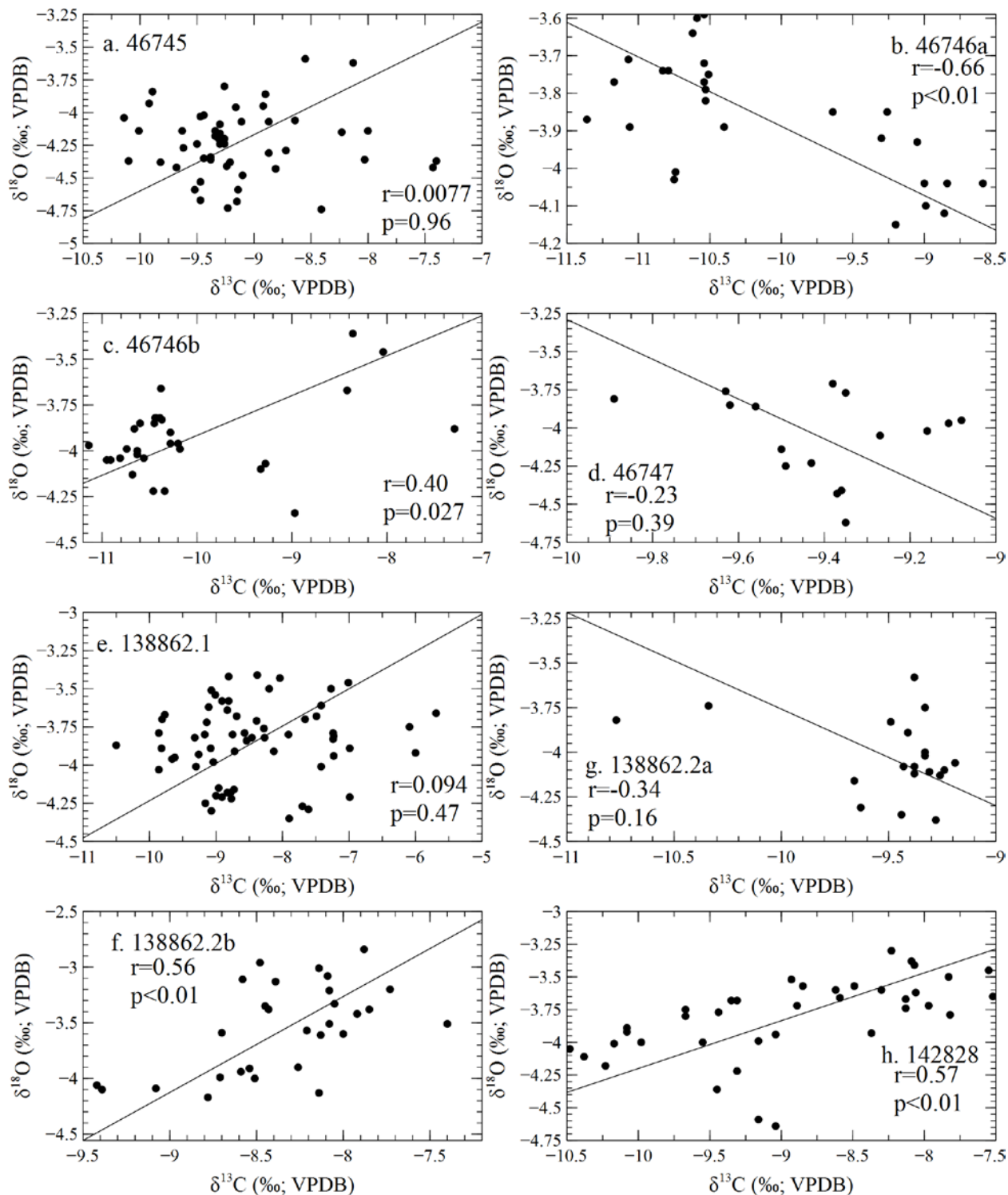
326 **Supplementary Figure 6:** Measured  $\delta^{18}\text{O}_c$  plotted against  $\delta^{13}\text{C}$  for samples from Staircase Cave.  
327 Regression lines were calculated using reduced major axis regression. Sample numbers, Pearson's  $r$  and  
328  $p$ -values are given in the graphs.



329

330

331 **Supplementary Figure 7:** Measured  $\delta^{18}\text{O}_c$  plotted against  $\delta^{13}\text{C}$  for samples from PP29. Regression lines  
 332 were calculated using reduced major axis regression. Sample numbers, Pearson's  $r$  and  $p$ -values are  
 333 given in the graphs.



334

335